Bias-switchable negative and positive photoconductivity in 2D $FePS_3$ ultraviolet photodetectors

Yi Gao[1,2,a], Shuijin Lei[3,a], Tingting Kang[4], Linfeng Fei[5], Jian Yuan[2,6], Mingguang Zhang[1], Shaojuan Li[6], Qiaoliang Bao[7], Zhongming Zeng[8*], Haoshuang Gu[1*] and Kai Zhang[2*]

[1]Hubei Collaborative Innovation Center for Advanced Organic Chemical Materials-Hubei Key Laboratory of Ferro & Piezoelectric Materials and Devices, Faculty of Physics & Electronic Sciences, Hubei University, Wuhan 430062, P. R. China

[2]*i*-Lab, Suzhou Institute of Nano-Tech and Nano-Bionics (SINANO), Chinese Academy of Sciences, Suzhou 215123, Jiangsu, P. R. China

[3]School of Materials Science and Engineering, Nanchang University, Nanchang 330031, Jiangxi, P. R. China

[4]State Key Laboratory of Infrared Physics, Shanghai Institute of Technical Physics, Chinese Academy of Sciences, Shanghai 200083, P. R. China

[5]Department of Applied Physics, The Hong Kong Polytechnic University, Hong Kong , P. R. China

[6]Institute of Functional Nano and Soft Materials (FUNSOM), Jiangsu Key Laboratory for Carbon-Based Functional Materials and Devices, Soochow University, 199 Ren'ai Road, Suzhou 215123, Jiangsu, P. R. China

[7]Department of Materials Science and Engineering, Faculty of Engineering, Monash University, Clayton 3800, Victoria, Australia

[8]Key Laboratory of Nanodevices and Applications, Suzhou Institute of Nano-Tech and Nano-Bionics (SINANO), Chinese Academy of Sciences, Suzhou 215123, Jiangsu, P. R. China

[a]These authors contributed equally to the work

[*]**Email:** zmzeng2012@sinano.ac.cn, guhsh@hubu.edu.cn and kzhang2015@sinano.ac.cn

Abstract:

Metal-phosphorus-trichalcogenides (MPTs), represented by $NiPS_3$, $FePS_3$ et al., are newly developed two-dimensional (2D) wide bandgap semiconductor and have been proposed to be splendid candidate for ultraviolet (UV) optoelectronics. Although with superior advantages for solar-blind UV photodetectors, including those of free of surface trap states, highly compatible with versatile integrations as well as appropriate bandgap, relevant study is rare up to date. In this work, photoresponse characteristic of UV detectors based on few-layer $FePS_3$ has been comprehensively investigated. The responsivity of the photodetector, which is observed to be determined by bias gate voltage, may achieve as high as 171.6 mAW^{-1} under the illumination of 254 nm weak light that is comparable to most commercial UV detectors. Notably, both negative and positive photoconductivities exist in the $FePS_3$ photodetectors and can be controllably switched with bias voltage. The eminent and novel photoresponse property paves way for the further development and practical use of 2D MPTs in high-performance UV photodetections.

Keywords: UV photodetector, 2D wide bandgap material, $FePS_3$, photoconductivity

Gao, Y., Lei, S., Kang, T., Fei, L., Mak, C. L., Yuan, J., ... & Zhang, K. (2018). Bias-switchable negative and positive photoconductivity in 2D FePS3 ultraviolet photodetectors. Nanotechnology, 29(24), 244001.

1. Introduction

Ultraviolet (UV) photodetectors are usually very sensitive in light detection with short wavelength (typically less than 400 nm), owning to their advantages of high wave-selectivity and low nature-light radiation.[1] This feature promises its broad applications ranging from military domain including missile early warning, secure optical communication to civilian use as environmental monitoring, biological and chemical analysis, etc.[2-4] In general, wide bandgap semiconductors like GaN,[5] ZnO,[6] SiC,[7] diamond and most recent Ga_2O_3[8] are appropriate candidates for UV-absorbing materials. However, the performance of wide bandgap semiconductor-based photodetectors currently encounter challenges of slow response and recovery speed causing from surface trap states.[9] In addition, the requirement of unavoidable epitaxy process hinders the compact integration and further development of devices based on these materials.

Compared with conventional semiconductor, two dimensional (2D) materials exhibit distinguished advantages in solving the above problems for photodetection applications. They are free of dangling bonds on the surface, which reduces the scattering centers and hence promises shortened response time by accelerating the photogenerated electron–hole pairs.[10] Furthermore, the atomic thick feature together with the possibility of van der Waals integration allows for high compatibility with versatile systems and microfabrication techniques.[11,12] Graphene and transition metal dichalcogenides (TMDCs) have been proposed and well developed for photodetectors.[13-15] Relatively small bandgap (E_g < 2 eV) of these materials limits their optoelectronic applications in UV regime. Although broadband response (including UV band) could be realized with modified graphene,[16] TMDCs[17] and their heterostructures,[18-20] the wave-selection is still a barrier in general. Developing 2D materials with suitable bandgap for UV photodetectors turns to be crucial. Wide-bandgap 2D semiconductors, thus, have attracted considerable interest in realizing reliable performance for UV detections with high detectivity and fast response when reserving the merit of 2D materials. Metal-phosphorus-trichalcogenides (MPTs), represented by $NiPS_3$, $FePS_3$ et al., are newly developed 2D semiconductor materials with similar atom structure as TMDCs while owning intrinsic large bandgap (up to 3.5 eV).[21] Because of the suitable bandgap and theoretically predicted high carrier mobility, MPTs are suggested to be splendid candidates for UV detectors but with rare report. Most recently, He et al. for the first time attempted a UV photodetector based on few-layer $NiPS_3$ nanosheets which shows remarkable photoresponse together with fast response speed.[22] There is still room for improving the metrics of MPTs-based UV photodetectors.

In this work, we comprehensively investigated the photoresponse of another novel MPTs member, $FePS_3$, which possesses 2 eV bandgap and a higher conductivity comparing to $NiPS_3$.[23,24] It was found that, despite the obvious sensitivity to deep UV light illumination (wavelength of 254 nm), the responsivity of the detector with few-layer $FePS_3$ was determined by bias voltage. More interestingly, both negative and positive photoconductivities exist and can be switched under bias control for the fabricated $FePS_3$ photodetectors. The correlated mechanism was also well clarified in illuminating the optimizing route for the practical use of 2D MPTs in high-performance UV photodetections.

2. Experimental details

2.1 Synthesis of $FePS_3$

A stoichiometric amount of high-purity elements (Fe: 99.99%, 1.221g; P: 99.999%, 0.677g; S: 99.99%, 2.102g) and 0.1 g of iodine as the transport agent were sealed into a quartz ampoule (15 cm in length and 1.5 cm in diameter) under vacuum, which was then set in a horizontal furnace over a temperature gradient from 700 °C to 630 °C. After heated for 2 weeks, the ampoule was cooled down to room temperature and the black plate-like crystals with metallic luster were formed in the deposition zone.

2.2 Material Characterizations

X-ray powder diffraction (XRD) patterns were recorded on a Rigaku SmartLab Intelligent X-ray diffraction system with filtered Cu Kα radiation (λ = 1.5406 Å, operating at 45 kV and 200 mA). Transmission electron microscopy (TEM) images, high resolution transmission electron microscopy (HRTEM) images, selected area electron diffraction (SAED) patterns, energy dispersive X-ray spectroscopy (EDS) elemental mapping were taken from a JEM-2100F (field emission) scanning transmission electron microscope (JEOL, Japan) with an acceleration voltage of 200 kV. Raman measurements were performed in a Horiba HR evolution, the excitation was provided by light (λ=532 nm) through a 100× objective.Thickness was measured with a atomic force microscope (Bruker Icon). A spectrophotometer (Lambda 750) was employed to acquire UV-Vis absorbtion spectra.

2.3 Device fabrication and measurements

To fabricate field-effect transistors (FETs), few-layered $FePS_3$ nanosheets were first obtained through a mechanical exfoliating method using a blue Nitto tape. Then the obtained sheets were transferred onto a Si/SiO_2 (285 nm) substrate by the commonly used dry transfer method.Optical microscope was used to select the samples with thickness of 10-20 nm. Atomic force microscope (Vecco Dimension3000) was used to confirm the thickness. Electron beam lithography (JEOL JBX 5500) was used to define source and drain electrode patterns, and Cr/Au (10/90 nm) film was deposited onto substrates using an electron bean evaporator (ULVAC Ei-5Z). The photodetectors have the same structure as the FETs mentioned above. All the measurements were performed in a vacuum probing station at room temperature with vacuum of 10^{-4} Pa. The data was collected with a Keithley 4200 semiconductor parameter analyzer. A light source with 254 nm wavelength was used to illuminate the devices. The power density was measured to be 0.18 mW/cm^2.

3. Results and discussion

The crystal structure of the synthesized $FePS_3$ is shown in **Figure 1**a. Generally, $FePS_3$ has the $CdCl_2$ type-structure[25] in which S atoms occupy the Cl sites forming layer lattices with

double layers, and one third of the Fe atoms are substituted by P-P pairs. Fe atoms and P-P pairs are filled in the octahedral centers of S-sublattice forming P_2S_6 bipyramid units. Each S atom bonded to a single P atom and two Fe atoms. In this case, Fe atoms and P-P pairs are sandwiched between the sulfur double layers resulting into lamellar structures. Therefore, it is often expressed as hexachalkogenohypodiphosphate, i.e. $3[SFe_{2/3}(P2)_{1/3}S] = Fe_2P_2S_6$. These layers are weakly bonded through Van der Waals S-S interactions, hence, a 2D nanostructure can be easily prepared by a clear method such as exfoliation. As shown in Figure 1b, a large amount of $FePS_3$ flakes with average size of ~3 mm can be obtained during synthesis. Figure 1c shows the atomic force microscope (AFM) image of the exfoliated few-layer $FePS_3$ nanosheet, the thickness of which is about 15 nm. Figure 1d shows the typical XRD patterns of the prepared sample. All the diffraction peaks can be readily indexed to the monoclinic structure of $FePS_3$ with the calculated lattice constants of a = 5.9484 Å, b = 10.2997 Å, c = 6.7215 Å and β = 107.16°, which are perfectly consistent with the reported data (JCPDS Card File No. 78−0496, a = 5.947 Å, b = 10.300 Å, c = 6.722 Å and β = 107.16°). No characteristic reflection peaks originated from other components such as iron sulfides, iron phosphides or corresponding elements, indicating the pure phase of $FePS_3$. Raman spectra were collected using a 532 laser in ambient condition. As shown in Figure 1e, 99.8, 157.2, 226.4, 247.5, 279.1, 380.1 cm^{-1} can be identified in both bulk and layered $FePS_3$, which is consistent with previous report.[21] The peaks ranging from 85-100 cm^{-1} originate from the Fe atom vibration in $FePS_3$[26]. The peak P_1 (99.8 cm^{-1}) in $FePS_3$ bulk shows broad line shape, could be decomposed into two or more peaks. The intensity of these decomposed peaks may be affected by the thickness of the sample[27]. In few-layered FePS3, the intensity of some decomposed peak become stronger and an extruded peak around 90.4 cm^{-1} would appear.

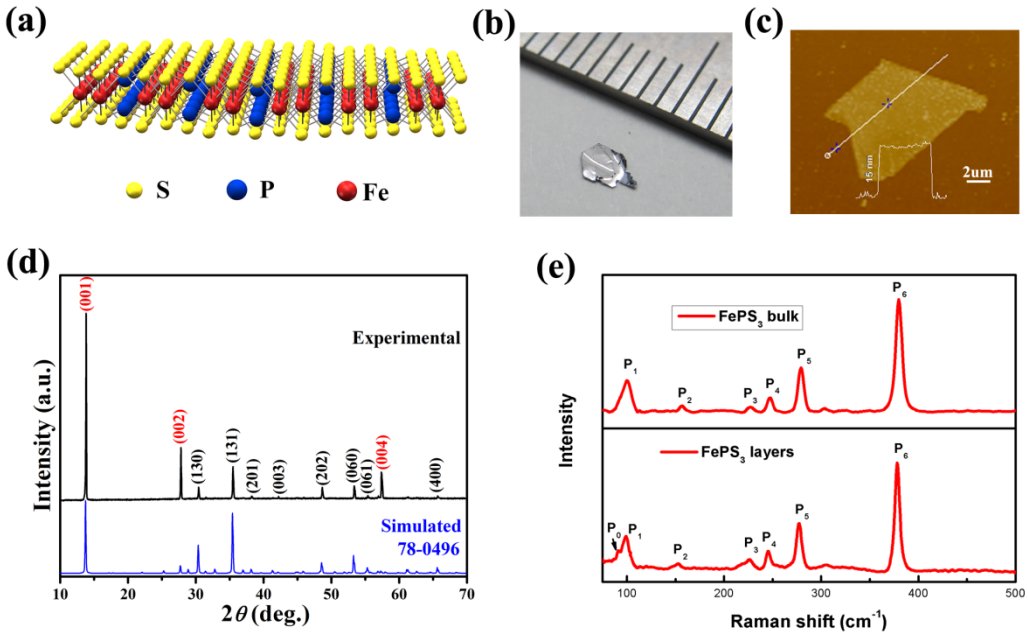

Figure 1. (a) Atomic structure of $FePS_3$. (b) Typical optical image of synthesized $FePS_3$ flakes. (c) AFM image of an exfoliated few-layer $FePS_3$ nanosheet with thickness of 15 nm. (d) XRD diffraction pattern of $FePS_3$ and their corresponding lattice planes. (e) Raman spectra of bulk and few-layered $FePS_3$.

To further evaluate the quality of the synthesized $FePS_3$, microstructure and chemical component analysis were carried out by employing TEM, SEAD and EDS. **Figure 2**a presents a typical TEM image of the obtained few-layer $FePS_3$ nanosheet sample, demonstrating the clear 2D nanosheet structures. The corresponding SAED patterns recorded along [001] zone axis also can be perfectly indexed as the monoclinic $FePS_3$ structure and the single-crystalline nature of the nanosheets (inserted in Figure 1a).To further investigate the microstructure of these $FePS_3$ nanosheets, HRTEM was performed. As displayed in Figure 2b, the HRTEM image exhibits two-dimensional atomic lattice fringes, suggesting a good crystallinity of the nanosheets. The three characterized interplanar spacings can be measured to be 0.28, 0.29 and 0.29 nm, which match well with the (200), (130) and $(\bar{1}30)$ planes of monoclinic structure of $FePS_3$ phase. As shown in Figure 2c-f, the EDS elemental mapping images exhibit a uniform distribution of Fe, P and S elements, further confirming the formation of $FePS_3$ phase.

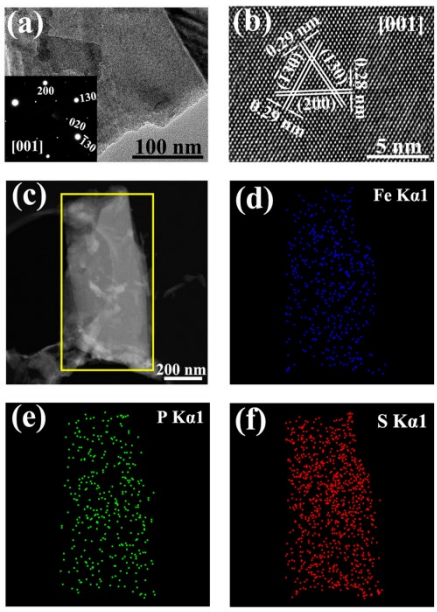

Figure 2. (a) A typical TEM micrograph of $FePS_3$ nanosheet and the inset shows the corresponding SEAD pattern. (b) The HRTEM image for the $FePS_3$ nanosheet. (c-f) The EDS element mapping images.

The measurements of electrical characteristic and photoresponse of the $FePS_3$ share the same FET device structure, with 254 nm wavelength light illumination as the optical source (schematically shown in **Figure 3**a). A typical profile of the device is given by the AFM scanning image in Figure 3b, where the thickness of the $FePS_3$ nanosheet is usually chosen to be ~10 nm. The output curves exhibit linear variations under different gate voltage bias (Figure 3c), which indicate a good ohmic contact between the $FePS_3$ nanosheet and metal electrodes. UV-Visible spectroscopy was used to measure the absorbance of the $FePS_3$ nanosheet (Figure 3d) and clear UV photoresponse characteristic can be observed, with much stronger absorption in the regime of wavelength less than 450 nm. Figure 3e shows the time dependence of photocurrent of a 11 nm-thick $FePS_3$ photodetector under a fixed V_{ds} of 60 mV and zero gate bias with a weak illumination of 254 nm wavelength light (power density ~ 0.18 mW/cm^2). It

is obvious that the photocurrent has a rapid decrease upon the illumination, representing a negative photoconductivity. The responsivity is a key factor to characterize the performance of photodetectors, which is defined as $R=I_{photo}/P_{incident}$, where, I_{photo} is the photocurrent and $P_{incident}$ is the incident power. At zero bias, R is calculated to be 12.3 mA W^{-1} for the as-prepared few-layer $FePS_3$ photodetector. And, the detector can be effectively switched on/off upon the switching of the illumination. As shown in Figure 3f, the rise and decay time of the device is very short with measured values of 105 ms and 120 ms respectively. Both the responsivity and response speed are comparable with most of detectors based on TMDCs.[28,29]

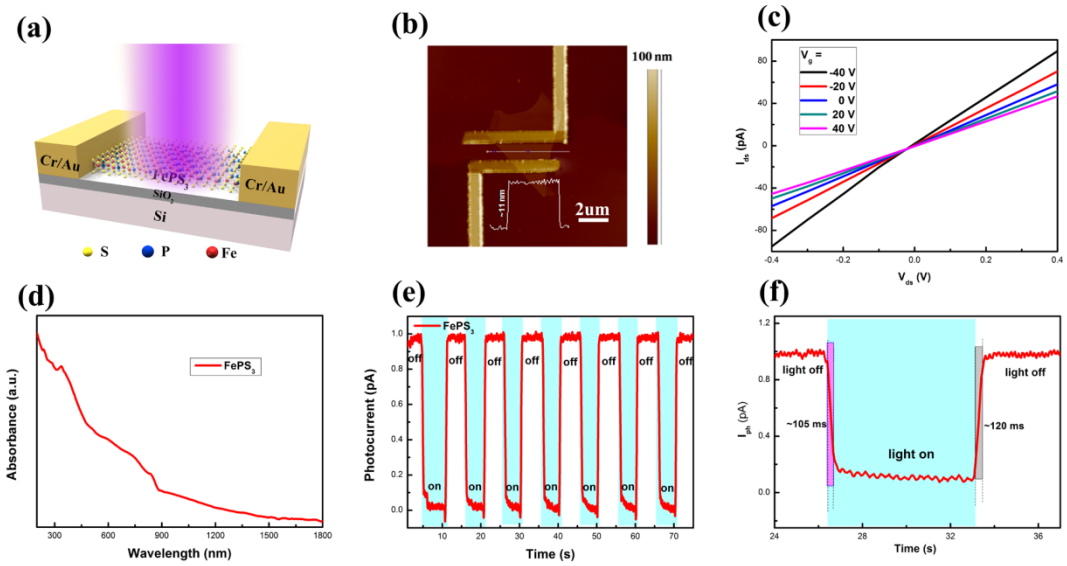

Figure 3. (a) Schematic diagram of a $FePS_3$ UV photodetector. (b) AFM image of a two-terminal FET device based on few-layer $FePS_3$ nanosheet with thickness of ~11 nm. (c) Output characteristics of the $FePS_3$ FET as a function of gate voltage bias ranging from -40 V to 40 V. (d) UV-Vis absorption spectrum of a typical few-layer $FePS_3$ nanosheet. (e) Time-dependent photocurrent of the $FePS_3$ photodetector. Incident light: 254 nm, V_{ds} = 60 mV, and V_g = 0 V. (f) Photoresponse time of the $FePS_3$ detector. The rise and decay time are 105 ms and 120 ms, respectively.

Gate voltage bias usually has significant impact on the photodetectors' performance, a series of discontinuous gate voltage bias were added to the device accordingly in our experiment to check the dependence. With the applying of gate voltage bias, the device displays tunable responsivity which depends on voltage bias. In addition, the device exhibits different response modes, namely positive photoconductivity (PEC) and negative photoconductivity (NEC) when turning the bias from negative gate voltage to positive ones. **Figure 4**a shows the generally statistic of the responsivities under different gate voltage bias. In the negative bias range, the responsivity increases exponentially with the decrease of bias, and reaches 171.6 mAW^{-1} when the voltage is -40 V, which has a more than 3 times enhancement relative to that at -20 bias and is comparable to the traditional UV detectors.[30,31] In the positive scope, the responsivity shows approximative linearization contrary to the increase of voltage bias. Figure 4b-d are specific time dependent responsivity measurements under different negative bias while Figure 4e-g show the responsivity details in different positive bias.

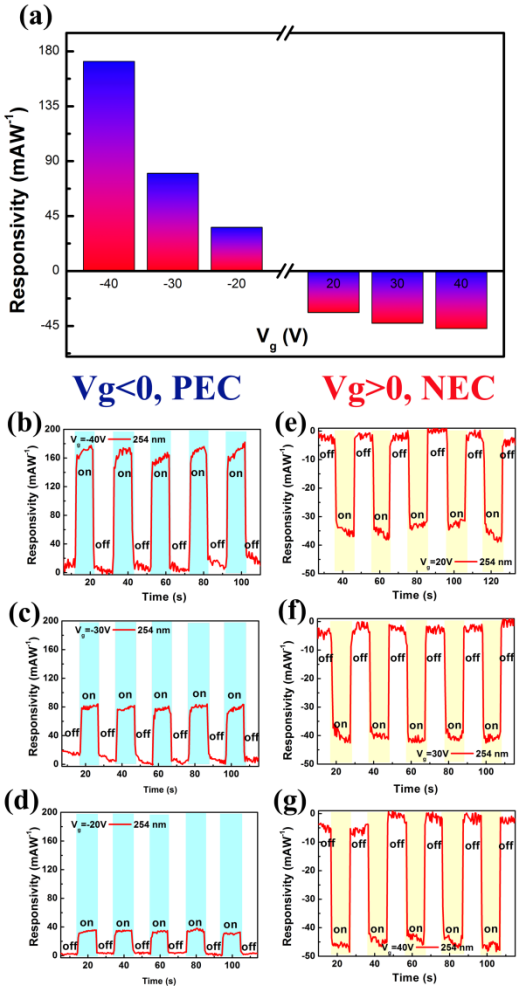

Figure 4. (a) General statistic of responsivity of a $FePS_3$ photodetector at different gate voltage bias. (b-d) Positive photoconductivity response under different negative bias. (e-g) Negative photoconductivity response under different positive bias.

It is novel and interesting that the photodetector displays two modes of photoconductivity response which are controllable by bias gate voltage. Exploring the internal mechanism is important and meaningful for the further optimization of MPTs-based UV photodetectors. **Figure 5**a shows transfer curves of the device with the illumination on and off as comparison. A fixed V_{ds} of 60 mV was supplied with Vg ranged from -40 V to 40 V ,under illumination of 245 nm (power density ~ 0.18 mW/cm^2). Besides the obvious p-type conduction mode, we can see clearly that the photocurrent changes more dramatically under illumination, which is much higher in negative part and decrease drastically to the lower standard when a positive bias is provided. The photocurrent is proportional to conductivity σ, For $FePS_3$, the hole concentration p and hole mobility μ_p play important roles in the process as a p-type semiconductor, according to the formula $\sigma = \mu \times p$ (with μ being mobility ration and p being hole concentration). The physical mechanism for the negative and positive photoresponsivity could be explained by the competition between μ_p and p. Figure 5b shows the decay of p under illumination. A p-type semiconductor is dominated by acceptor levels, but the minority carrier and corresponding energy level induced by defects[32], co-doping[33], hydrogen sorption[34], and

interface impurities[35] can also play important roles in devices[36]. As for $FePS_3$, the donor energy level could be brought in by CVT induced defects, possible O dangling bonds on SiO_2 surface, hydrogen absorption[37] and replacement between P atom and S atom. When the light is on, some electrons on donor level (E_d) absorb the photon energy and are excited to the conduction band, corresponding to the process ❶. Then the process ❷occurs, the photon-excited electrons will recombine with holes on valence band, thus reducing the hole concentration. Figure 5c shows the variation of μ_p according to bias. With light on, holes on Fermi level (E_f) were excited to E_v. Subtracting the energy difference between E_v and E_f, the remaining photon energy will left for the photo-excited hole's kinetic energy. And it is reasonable that the hole's mobility will be higher for higher hole kinetic energy, as shown in Figure 5c (left). When more negative bias is applied, E_f will shift down towards E_v, leaving more energy and higher mobility for the photo-excited holes.[30] In this sense, the higher bias was provided, the higher μ_p was obtained.

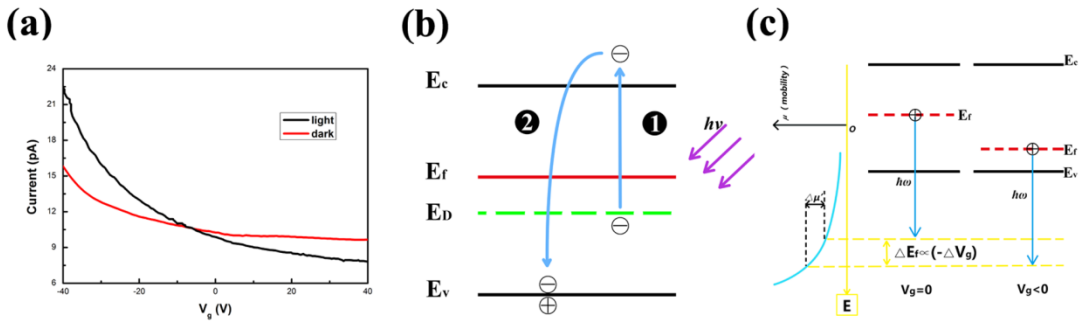

Figure 5. (a) Transfer curve of the $FePS_3$ photodetection device with and without illumination. Light wavelength: 254 nm, V_{ds}= 60 mV. (b) Processes show the decaying of hole concentration. (c) Gate voltage bias adjust Fermi level, leading the difference in hole mobility.

4. Conclusion

In summary, a typical 2D wide bandgap semiconductor, $FePS_3$ flakes with high crystalline and uniformity were synthesised. The gate bias voltage regulation of few-layer $FePS_3$ UV detectors demonstrate an impressive performance. The response and decay time of the detector is as fast as 105 ms and 120 ms, respectively. Under weak illumination, the responsivity has an obvious enhancement with bias voltage and reaches 171.6 mAW^{-1} at -40V. In addition, the detector manifests a novel photoresponse characteristic which behaves a switch of positive photoconductivity to negative photoconductivity with the change of gate voltage bias. This eminent and novel property may illuminate the further optimization of the MPTs-based UV photodetectors.

Acknowledgements

This work was supported by the National Natural Science Foundation of China (Grant No. 11574349, 11474088, 51732010), the Natural Science Foundation of Jiangsu province (Grant Nos. BK20150365, BK20170424) , the Natural Science Foundation of Hubei province (Grant No. 2016CFA081), the Key Research Program of Frontier Sciences of Chinese Academy of

Sciences (QYZDB-SSW-SLH031), and the Hundred Talent Program of Chinese Academy of Sciences. S.L. acknowledges the financial supports from the National Natural Science Foundation of China (21461014), the Project for Young Scientist Training of Jiangxi Province (20153BCB23022), and the Natural Science Foundation of Jiangxi Province (20151BAB206016).

References

[1] L. Su, Y. Wei, C. Jian, H. Chen and X. Fang, *Small* 2017, 13, 1701687.
[2] Y. Taniyasu, M. Kasu and T. Makimoto, *Nature* 2006, 441, 325.
[3] P. Fan, U. K. Chettiar, L. Cao, F. Afshinmanesh, N. Engheta and M. L. Brongersma, *Nat. Photonics* 2012, 6, 380.
[4] S. M. Hatch, J. Briscoe and S. Dunn, *Adv. Mater.* 2013, 25, 867.
[5] X. Fang *et al.*, *Appl. Mater. Interfaces* 2016, 8, 1661.
[6] A. K. Pal, and D. B. Mohan, *Nanotechnology* 2017, 28, 415707.
[7] G. Wolfowicz, C. P. Anderson, A. L. Yeats, S. J. Whiteley, J. Niklas, O. G. Poluektov, F. J. Heremans, D. D. Awschalom, *Nat. Commun*. 2017, 8, 1876.
[8] S. Oh, C. Kim, J. Kim, *ACS Photonics* 2017, DOI: 10.1021/acsphotonics.7b01486.
[9] R. Vetury, N. Q. Zhang, S. Keller, U. K. Mishra, *IEEE Trans Electron* 2001, 48, 560.
[10] F. Zhang, J. Appenzeller, *Nano Lett.* 2014, 15, 301.
[11] Z. Liu, S. P. Lau, F. Yan, *Chem. Soc. Rev.* 2015, 44, 5638.
[12] S. Vaziri, G. Lupina, C. Henkel, A. D. Smith, M. Östling, J. Dabrowski, G. Lippert, W. Mehr, M. C. Lemme, *Nano Lett.* 2013, 13, 1435.
[13] T. Mueller, F. Xia, and P. Avouris, *Nat. Photonics* 2010, 4, 297.
[14] W. Yu, S. Li, Y. Zhang, W. Ma, T. Sun, J. Yuan, K. Fu and Q. Bao, *Small* 2017, 13, 1700268.
[15] T. M. Chen, X. J. Wu, J. X. Wang, and G. W. Yang, *Nanoscale* 2017, 9, 11806.
[16] S. Du *et al.*, *Adv. Mater.* 2017, 29, 1700463.
[17] W. Choi, M. Cho, A. Konar, J. Lee, G. Cha, S. Hong, S. Kim, J. Kim, D. Jina, J. Joo, S. Kim, *Adv. Mater.* 2012, 24, 5832.
[18] M. Long *et al.*, *Nano Lett.* 2016, 16, 2254.
[19] J. Yan et al., *Chem Eur J* 2016, 22, 4764.
[20] J. Yang, H. Kwak, Y. Lee, Y. Kang, M. Cho, J. Cho, Y. Kim, S. Jeong, S. Park, H. Lee, and H. Kim, *Appl. Mater. Interfaces* 2016, 8, 8576.
[21] K. Du, X. Wang, Y. Liu, P. Hu, M. Utama, C. Gan, Q. Xiong, and C. Kloc, *ACS Nano* 2016, 10, 1738.
[22] J. Chu *et al.*, *Adv. Funct. Mater.* 2017, 27, 1701342.
[23] V. Grasso, F. Neri, S. Santangelo, and L. Silipigni, *Phys. Rev. B* 1988, 37, 4419.
[24] V. Manríquez, P. Barahona, O. Peña, *Mater. Res. Bull.* 2000, 35, 1889.
[25] S. Gundersen, A. Haaland, K. -G. Martinsen, and S. Samdal, *J. Mol. Struct.* 1994, 318, 251.
[26] M. Bernasconi, G. L. Marra, G. benedek, L. Miglo, M. Jouanne, C. Julien, M. Scagliotti, M. Balkanski, *Phys. Rev. B* 1988, 38, 12089.
[27] J. U. Lee, S. Lee, J. H. Ryoo, S. Kang, T. Y. Kim, P. Kim, C-H. Park, J-G. Park, and H.

Cheong, *Nano Lett.* 2016, 16, 7433.
[28] O. Lopez-Sanchez, D. Lembke, M. Kayci, A. Radenovic, and A. Kis, *Nat. Nanotechnology* 2013, 8, 497.
[29] W. Zhang, M. Chiu, C. Chen, W. Chen, L. Li, and A. T. S. Wee, *ACS Nano* 2014, 8, 8653.
[30] R. Zhuo, Y. Wang, D. Wu, Z. Lou, Z. Shi, T. Xu, J. Xu, Y. Tian and X. Li, *J. Mater. Chem. C* 2018, 6, 299.
[31] A. Gundimeda, S. Krishna, N. Aggarwal, A. Sharma, N. D. Sharma, K. K. Maurya, S. Husale, and G. Gupta, *Appl. Phys. Lett* 2017, 110, 103507.
[32] S. Samson, and C. G. Fonstad, J. Appl. Phys. 1973, 44, 4618.
[33] K. Arai, H. Namikawa, K. Kumata, and T. Honda, J. Appl. Phys. 1986, 59, 3430.
[34] P. D. C. King, et al, Phys. Rev. B 2009, 80, 081201.
[35] K. Dolui, I. Rungger, and S. Sanvito, Phys. Rev. B 2013, 87, 165402.
[36] L. F. J. Poper, T.D. Veal, C. F. McConville, H. Lu, and W. J. Schaff, Appl. Phys. Lett. 2006, 88, 252109.
[37] N. Ismail, A. A. El-Meligi, Y. M. Temerk, M. Madian, Int. J. Hydrogen. Energ. 2010, 35, 7827.
[38] K. V. Klitzing, G. Dorda, and M. Pepper, *Phys. Rev. Lett*, 1980, 45, 494.